

# Crystalline-state $\beta$ – $\alpha$ photoisomerization of cobaloxime complexes, part 1 Generation of asymmetry in chiral crystal environment

Akiko Sekine <sup>\*</sup>, Hiroaki Tatsuki, Yuji Ohashi

*Department of Chemistry, Tokyo Institute of Technology, Ookayama, Meguro-ku, Tokyo 152, Japan*

Received 15 July 1996; accepted 27 August 1996

## Abstract

The  $\beta$ -cyanoethyl groups bonded to the cobalt atoms in [ $\beta$ -cyanoethyl](3-methylpyridine)bis(dimethylglyoximate)cobalt(III) and [ $\beta$ -cyanoethyl](4-methylpyridine)bis(dimethylglyoximate)cobalt(III) are isomerized to the  $\alpha$ -cyanoethyl groups, at room temperature and at 346 K respectively, on exposure to visible light with retention of the single crystal form. The produced  $\alpha$ -cyanoethyl group has a chiral carbon atom bonded to the cobalt atom. The crystal structures of the 3-methylpyridine complex before and after the irradiation, which were determined by X-rays, revealed that the ratio of the *R* and *S* configurations of the produced  $\alpha$ -cyanoethyl group in one site was not 1:1 but about 4:7. On the other hand, the  $\alpha$ -cyanoethyl group only had the *R* configuration in one site of the 4-methylpyridine complex crystal. The difference in shape of the reaction cavities for the produced  $\alpha$ -cyanoethyl groups of the two complex crystals well explains the reason why such different degrees of asymmetry were generated in the produced  $\alpha$ -cyanoethyl groups. © 1997 Published by Elsevier Science S.A.

*Keywords:* Cobalt; Cobaloxime; Chiral crystal; Photoisomerization; Crystal structure

## 1. Introduction

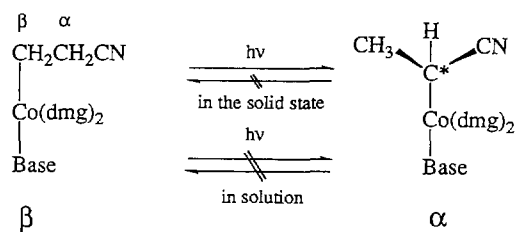
It has been found that the chiral alkyl group bonded to the cobalt atom in some bis(dimethylglyoximate)cobalt(III), cobaloxime, complex crystals is racemized on exposure to X-rays or visible light with retention of the single crystal form [1,2]. The rate of the racemization was well explained by the void space around the reactive group, reaction cavity, in each crystal structure [3]. When the racemic crystals were grown from a solution containing the racemic compound, the crystal exhibited a racemic-to-chiral transformation on exposure to X-rays or visible light, and when the transformed crystals were dissolved in a solution, the solution showed a significant optical rotation [4,5]. Although these findings are very important in analyzing the reaction mechanism, the reactions were limited to the racemization of chiral alkyl groups. In order to analyze the reaction mechanism more quantitatively, a variety of reactions should be observed as

crystalline-state reactions, for which the structural changes were observed by the stepwise structure analyses.

Recently it was reported that the  $\beta$ -cyanoethyl ( $\beta$ -ce) group bonded to the cobalt atom in some cobaloxime complexes was isomerized to the  $\alpha$ -cyanoethyl ( $\alpha$ -ce) group upon exposure to visible light [6], as shown in Scheme 1. The photoreaction,  $\beta$ – $\alpha$  photoisomerization, proceeds only in the solid state, and the reverse reaction has not been observed. A series of cobaloximes with different axial base ligands has been prepared and the relation between the reactivity and the reaction cavity has been examined [7–10]. In previous papers [11,12], it was proposed that the reaction rate depends on three factors in the initial crystal structure, that is cavity size, topochemical factors and the hydrogen bond of the reactive group. Since all the above crystals were decomposed during the isomerization, the isomerization retaining the single crystal form is more favorable for quantitative discussion.

Among the above cobaloxime complexes, it was found that the  $\beta$ -ce complex with 3-methylpyridine

<sup>\*</sup> Corresponding author.



Scheme 1.

(3mp) as an axial base ligand formed a mixed crystal with the  $\alpha$ -ce complex in a wide range of population. The structure of the mixed crystal is isomorphous to the  $\beta$ -ce complex crystal. The rate of isomerization of the mixed crystal is much faster than that of the  $\beta$ -ce complex crystal. This is due to the difference in cavity size of the ce groups between the  $\beta$ -ce complex crystal and the mixed one [13]. These facts strongly suggested that the  $\beta$ -ce crystal should be isomerized to the  $\alpha$ -ce crystal without degradation of the crystallinity.

After many trials, we found that the cell dimensions were gradually changed using a new type of Xe lamp with high flux and a glassfiber tube which brought the light to the crystal mounted on a diffractometer. The

analyzed structure clearly indicated that the  $\alpha$ -ce group appeared at the position of the  $\beta$ -ce group as a disordered structure.

Another  $\beta$ -ce complex with 4-methylpyridine (4mp) as an axial base ligand was also examined. This crystal exhibits a reversible phase transition with retention of the crystallinity at 343 K. In the low temperature phase, the crystal has two crystallographically independent molecules in the unit cell. After the phase transition the length of the  $c$  axis is reduced to one-half of its initial value and only one molecule is in the unit cell [14]. The structure of the high temperature phase is similar to that of 3mp complex. Therefore, the 4mp crystal was warmed to 346 K and exposed to the Xe lamp. The  $\beta$ -ce group was gradually changed to the  $\alpha$ -ce group with near retention of the crystallinity.

The produced  $\alpha$ -ce group after the isomerization has a chiral carbon atom bonded to the cobalt atom as shown in Scheme 1. In either crystal of 3mp or 4mp, to our surprise, the produced  $\alpha$ -ce group at one site is not racemic but one enantiomer of the  $\alpha$ -ce group has a larger population than the other. Although the other enantiomer is produced in the same population at another site related by a center of symmetry because of

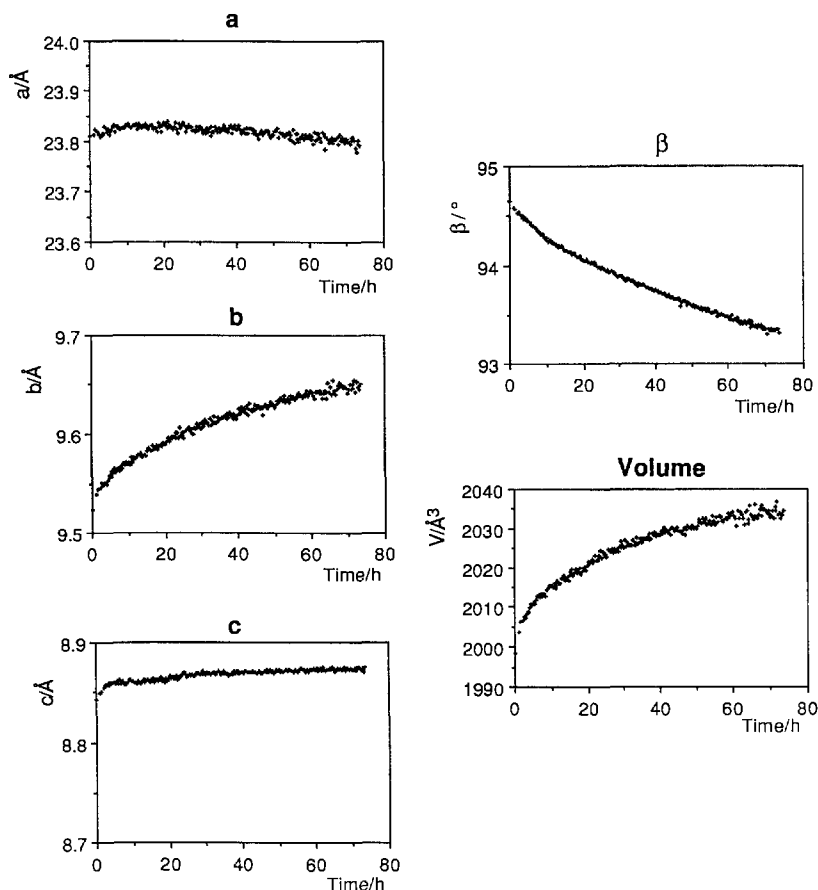


Fig. 1. Change of cell dimensions with exposure time for 3mp at 296 K.

the centrosymmetric space group of these crystals, this means the asymmetry is generated in a chiral crystal environment. Although the asymmetric syntheses in chiral crystals have been reported [15–18], it may probably be the first time that the generation of asymmetry has been observed as a crystalline-state reaction. This paper reports these new findings of crystalline-state photoisomerization and the generation of asymmetry in chiral crystal environments.

## 2. Experimental

### 2.1. Preparation

The  $\beta$ -ce complexes of 3mp and 4mp were prepared by the method reported previously [19,20]. The orange plate-like crystals of both complexes were obtained from hot methanol solutions.

### 2.2. $\beta$ - $\alpha$ photoisomerization of 3mp crystal

The crystal of 3mp was irradiated with an Xe lamp (Ushio UXL-5S + UI-501C) without any cut-off filter at the focusing position (the illuminance is  $180\,000\ 1 \times$ ) for 1 week. The cell dimensions were determined after

the exposure, but no change was observed except that the peak intensities of reflections were significantly decreased. Then a crystal was kept in an  $N_2$  laser beam for 20 h. The cell dimensions changed significantly, but the structure analysis did not show any change of the  $\beta$ -ce group. This result may indicate that the crystalline-state isomerization would be observed if the crystal was exposed to a stronger light source. Also, the measurements of cell dimensions at a constant interval are necessary during the irradiation in order to control the reaction rate.

A new type of Xe lamp with high flux (San-ei Super Bright 150) was used without any cut-off filter for the light source (the illuminance is more than  $1\,000\,000\ 1 \times$ ). The light was brought to the crystal mounted on a four-circle diffractometer using a 10 mm diameter glass-fiber tube. The top of the tube was placed at a distance of 10 mm from the crystal. The temperature at the crystal position was nearly the same as room temperature, which was examined before the experiment using thermocouples at the crystal position. The cell dimensions were measured at an interval of about 30 min. Fig. 1 shows the change of cell dimensions. Significant changes were observed for  $b$ ,  $\beta$  and unit cell volume  $V$ . Crystal data before and after the irradiation are given in Table 1.

Table 1  
Crystal data and experimental details

	3mp before irradiation	3mp after irradiation	4mp before irradiation	4mp after irradiation
$a/\text{\AA}$	23.756(3)	23.760(24)	32.056(5)	31.797(5)
$b/\text{\AA}$	9.525(2)	9.650(2)	8.897(4)	8.970(4)
$c/\text{\AA}$	8.822(2)	8.852(2)	8.842(6)	8.829(6)
$\beta/\text{deg}$	94.58(2)	93.28(6)	126.15(2)	125.79(2)
$V/\text{\AA}^3$	1989.9(7)	2026(2)	2036(2)	2042(2)
$Z$	4	4	4	4
Space group	$P2_1/a$	$P2_1/a$	$P2_1/a$	$P2_1/a$
Radiation	Mo K $\alpha$	Mo K $\alpha$	Mo K $\alpha$	Mo K $\alpha$
Wavelength/ $\text{\AA}$	0.71069	0.71069	0.71069	0.71069
Temperature/K	296	296	346	346
Crystal colour	orange	orange	orange	orange
Crystal size/ $\text{mm}^3$	$0.3 \times 0.3 \times 0.3$	$0.3 \times 0.3 \times 0.3$	$0.5 \times 0.5 \times 0.3$	$0.4 \times 0.3 \times 0.1$
Diffractometer type	AFC-5R	AFC-5R	AFC-5R	AFC-5R
Collection method	$\omega$ - $2\theta$ scan	$\omega$ - $2\theta$ scan	$\omega$ scan	$\omega$ scan
Absorption correction	no correction	no correction	no correction	no correction
$F_o$ limit (greater than)	$3\sigma$	$4\sigma$	$3\sigma$	$3\sigma$
$R$	0.044	0.113	0.056	0.083
$R_w$	0.050	—	0.062	0.080
$wR2$	—	0.303	—	—
$S$	1.69	1.01	2.15	1.71
Weighting scheme	$[\sigma^2(F)]^{-1}$	$[\sigma^2(F)]^{-1}$	$[\sigma^2(F)]^{-1}$	$[\sigma^2(F)]^{-1}$
$(\Delta/\sigma)_{\text{max}}$	0.1	0.01	0.06	0.19
$(\Delta\rho)_{\text{min}}$ ( $e^- \text{\AA}^{-3}$ )	-0.3	-0.8		
$(\Delta\rho)_{\text{max}}$ ( $e^- \text{\AA}^{-3}$ )	0.3	0.7		
No. of reflections used in refinement	3081	3558	2455	1625
No. of parameters refined	353	258	277	220

### 2.3. Crystal structure analyses of 3mp before and after the irradiation

The three-dimensional intensity data for the 3mp crystal were collected before and after the irradiation. The crystal structure before irradiation was substantially the same as that reported previously [7]. When the crystal was exposed to the Xe lamp for 74 h the change of cell dimensions became significantly small, as shown in Fig. 1. Since the intensities of reflections decreased significantly owing to the slow decomposition of the crystal after 74 h exposure, the irradiation was stopped and the three-dimensional intensity data were collected. The experimental details for the data collection are

given in Table 1. The crystal structure after 74 h exposure was solved by the direct method using the program MITHRIL [21].

Several new peaks appeared around the  $\beta$ -ce group on a difference map for the crystal after exposure. The peaks were assigned to the  $\alpha$ -ce groups with *R* and *S* configurations produced by  $\beta$ - $\alpha$  photoisomerization. The structure was refined by full-matrix least squares using the program SHELXL93 [22]. The occupancy factors of the  $\beta$ -ce group and the  $\alpha$ -ce groups with *R* and *S* configurations were converged to 0.45(4) and 0.19(4) and 0.36(4) respectively. The anisotropic temperature factors were applied for non-hydrogen atoms except for the  $\alpha$ - and  $\beta$ -ce groups, which were refined isotropi-

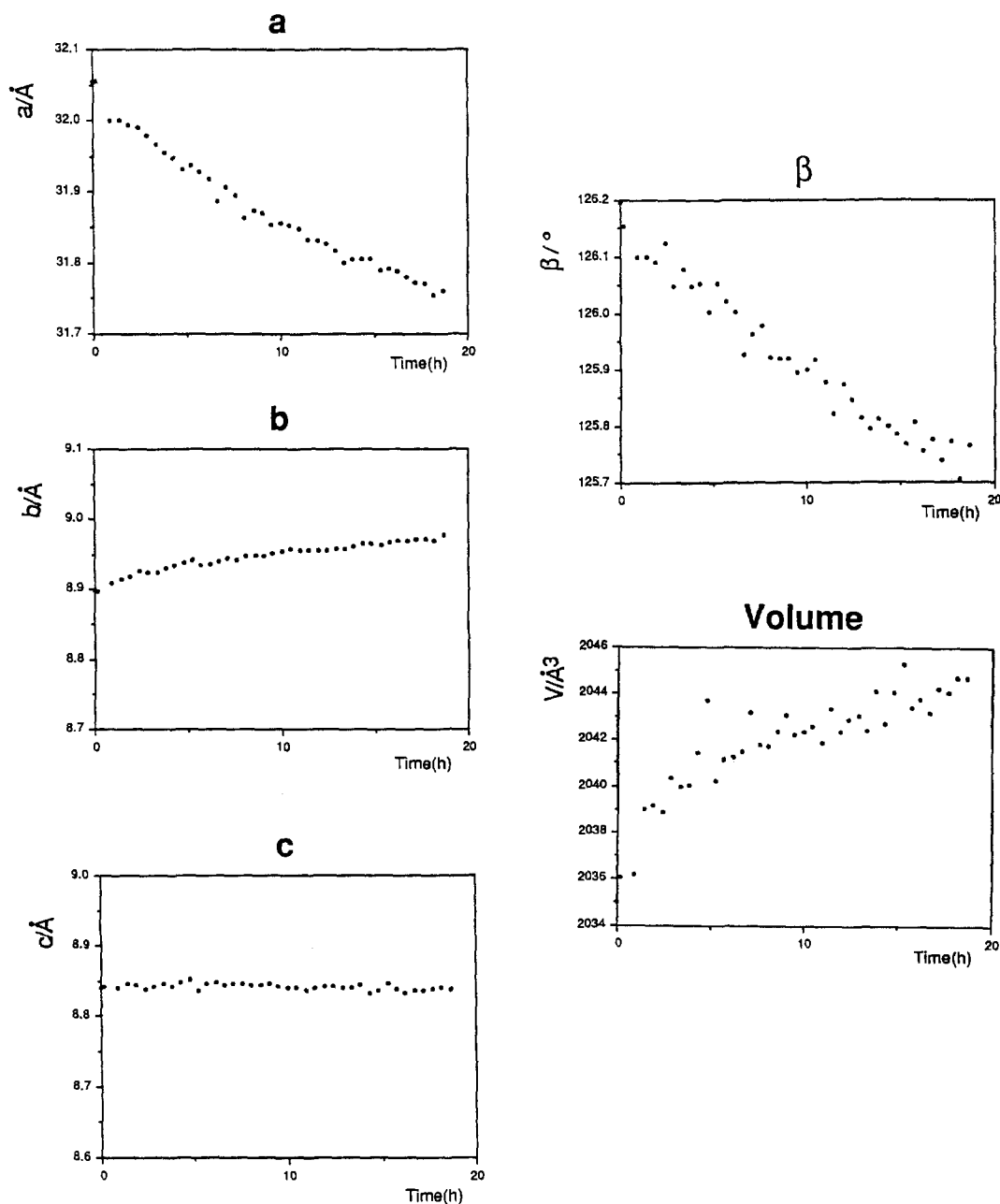


Fig. 2. Change of cell dimensions with exposure time for 4mp at 346 K.

cally. The hydrogen atoms, except the disordered ones, were obtained geometrically and refined with the isotropic thermal factors. Other details of the refinement are also given in Table 1.

#### 2.4. Cell change and crystal structure analyses of 4mp at 346 K

A crystal of 4mp was mounted on an AFC-4 diffractometer and was warmed to 346 K with the hot-air-flow method. The three-dimensional intensity data were collected in a way similar to that for the 3mp crystal. The analyzed structure is substantially the same as that reported previously [14]. The crystal was irradiated with the Xe lamp in the same way as that for the 3mp crystal. The cell dimensions were measured at an interval of about 30 min. Fig. 2 shows the change of cell dimensions with the exposure time. After 18 h the change became significantly small and the crystal was gradually decomposed. The three-dimensional intensity data were collected. The crystal data and experimental details are also summarized in Table 1. Tables of bond lengths and angles, anisotropic thermal parameters and hydrogen atom coordinates have been deposited at the Cambridge Crystallographic Data Centre.

The structure after irradiation was solved by the direct method using the program MITHRIL. The occupancy factors of the  $\beta$ -ce and  $\alpha$ -ce groups were estimated to have the same average isotropic temperature factors. The refinement was performed with the program TEXSAN [23]. They were 0.7 and 0.3 for the  $\beta$ -ce and  $\alpha$ -ce groups respectively. All the non-hydrogen atoms except C17B, C15B and N6B were refined with anisotropic temperature factors. The C17B, C15B and N6B atoms were refined isotropically. After several cycles of the refinement, the disordered atoms, N6A, N6B, C15A, C15B, C16A, C17A, and C17B, were not refined, since the geometry of the disordered cyanoethyl group was distorted. All the positions of the hydrogen atoms except those bonded to C15A were calculated geometrically but not refined. Other details of the refinement are given in Table 1. Tables of bond lengths and angles, anisotropic thermal parameters and hydrogen atom coordinates have been deposited at the Cambridge Crystallographic Data Centre.

Atomic scattering factors including anomalous terms were taken from Ref. [24]. The calculations were carried out on the VAX station 3100 and Sparc station 10 computers of our laboratory.

### 3. Results

#### 3.1. Change of cell dimensions of 3mp and 4mp

Fig. 1 shows the change of cell dimensions for the 3mp crystal. The log plot of the change of  $V$  with

exposure time is shown in Fig. 3. The conversion at any point of time was obtained assuming that the conversion at 74 h exposure is 0.55. The rate constant in the early stages was calculated to be  $1.3 \times 10^{-5} \text{ s}^{-1}$ , assuming first-order kinetics. The other dimensions were not so clear since the changes were not so large. Since the change of the 4mp crystal differs significantly from first-order kinetics, the rate constant was not calculated.

#### 3.2. Change of crystal and molecular structure of 3mp

The atomic parameters for non-hydrogen atoms of the 3mp crystal after the irradiation with their estimated standard deviations are given in Table 2. The crystal structures before and after the irradiation, shown in Fig. 4, are essentially the same as each other except the atoms appeared around the  $\beta$ -ce group, which were assigned to the atoms of the  $\alpha$ -ce groups with  $R$  and  $S$  configurations. The molecular structures of 3mp complexes with the numbering atoms before and after irradiation are compared in Fig. 5. Recently the racemic crystals of 3mp were prepared and their crystal structures were analyzed [25]. The molecular structure observed in the racemic 3mp complex, which is shown in Fig. 6, is very similar to that produced in the photoisomerization shown in Fig. 5(b). The conformation of the  $\beta$ -ce group is approximately the same before and after the irradiation. The population of the produced  $\alpha$ -ce and the original  $\beta$ -ce complexes are 0.55(4) and 0.45(4) respectively. The produced  $\alpha$ -ce group is not racemic. The occupancy factors of the methyl groups of  $S$  and  $R$  configurations produced, C10A and C10B, are 0.36(4) and 0.19(4) respectively. The ratio is approximately 7:4. The bond distances and angles after the irradiation are not significantly different from the corresponding ones before the irradiation, except the produced  $\alpha$ -ce group.

#### 3.3. Change of crystal and molecular structure of 4mp

The atomic parameters for non-hydrogen atoms of the 4mp crystal at 346 K before and after the irradiation

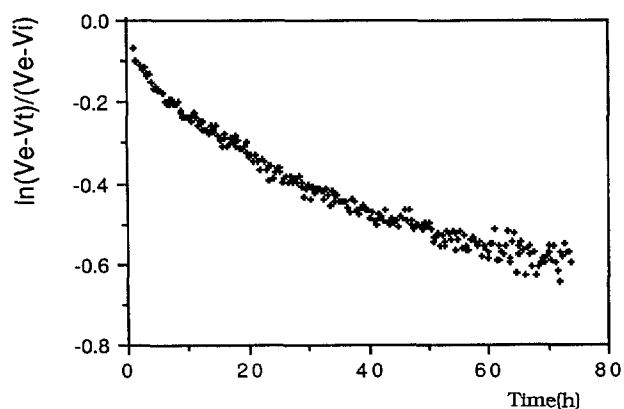


Fig. 3. Log plots of the change of  $V$  with exposure time for 3mp at 296 K.

Table 2

Final atomic coordinates ( $\times 10^4$ ) and equivalent isotropic thermal parameters ( $\times 10^3$ ) for 3mp after irradiation

	<i>x</i>	<i>y</i>	<i>z</i>	<i>U</i> <sub>eq</sub>
Co(1)	6374.7(6)	1755(2)	7869(2)	45(1)
O(1)	6723(4)	763(8)	5018(8)	59(2)
O(2)	6459(4)	4467(8)	9067(9)	70(3)
O(3)	6049(4)	2735(9)	10727(9)	70(3)
O(4)	6309(4)	-1006(7)	6705(9)	60(2)
N(1)	6678(4)	1864(9)	5944(10)	51(2)
N(2)	6549(4)	3680(9)	7866(10)	53(2)
N(3)	6073(4)	1617(10)	9783(10)	54(2)
N(4)	6190(4)	-127(9)	7850(10)	52(2)
C(1)	6813(5)	3079(12)	5501(13)	54(3)
C(2)	6759(5)	4146(11)	6678(15)	57(3)
C(3)	5894(5)	422(13)	10194(11)	55(3)
C(4)	5965(5)	-640(11)	9053(12)	50(3)
C(5)	7051(6)	3420(13)	4005(14)	72(4)
C(6)	6925(7)	5668(13)	6509(18)	85(4)
C(7)	5669(6)	147(14)	11714(12)	66(3)
C(8)	5811(7)	-2109(12)	9249(15)	74(4)
C(9)	7105(7)	1044(22)	8806(37)	77(5)
C(10)	7593(11)	1980(36)	9226(33)	124(15)
C(11)	7915(12)	2392(51)	7942(33)	91(13)
N(5)	8170(15)	2710(42)	7004(35)	105(11)
C(9A)	7177(5)	1404(19)	8881(21)	77(5)
C(10A)	7298(18)	27(24)	9501(45)	88(12)
C(11A)	7603(8)	1987(22)	7977(22)	56(5)
N(5A)	7973(12)	2467(40)	7375(40)	105(9)
C(10B)	7241(34)	1408(87)	10531(22)	84(23)
N(6)	5602(4)	2248(8)	6907(9)	43(2)
C(12)	5280(5)	3300(11)	7454(11)	49(3)
C(13)	4770(6)	3661(12)	6822(15)	64(3)
C(14)	4571(5)	2989(15)	5513(16)	74(4)
C(15)	4901(6)	1985(13)	4931(14)	66(3)
C(16)	5399(5)	1621(13)	5636(11)	53(3)
C(17)	4441(8)	4845(15)	7505(18)	98(5)

$$U_{eq} = (1/3)\sum_i \sum_j U_{ij} a_i^* a_j^* \cdot a_i \cdot a_j$$

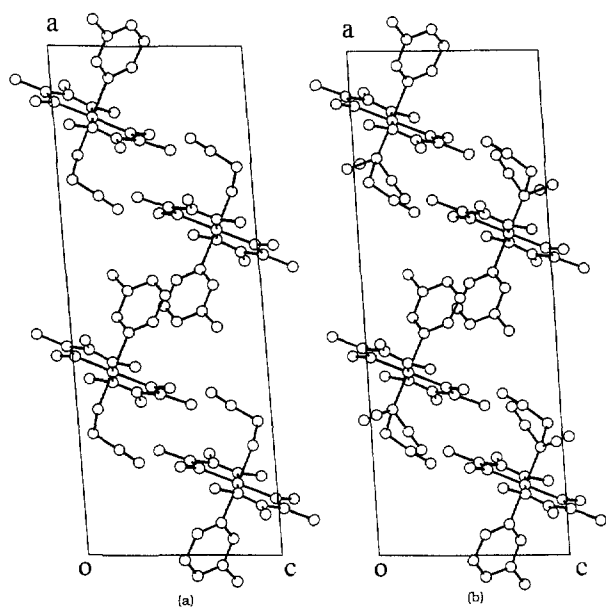


Fig. 4. Crystal structures of 3mp viewed along the *b* axis (a) before and (b) after the irradiation.

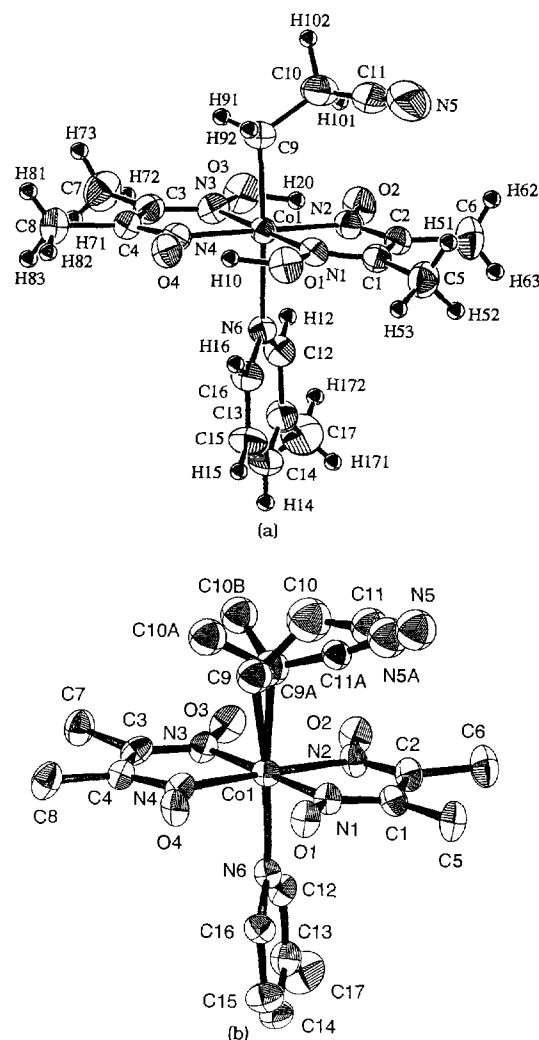


Fig. 5. Molecular structures of 3mp with numbering atoms (a) before and (b) after irradiation. The thermal ellipsoids are drawn at the 30% probability level. In (b) the H atoms are omitted for clarity.

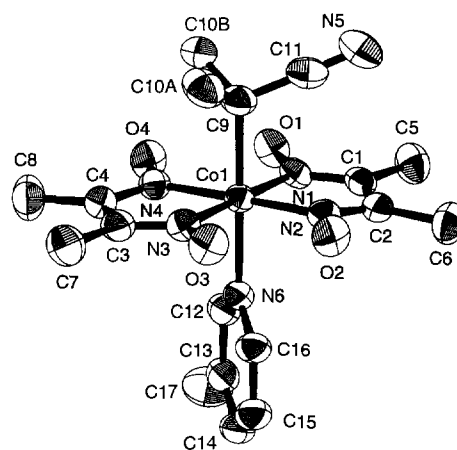


Fig. 6. Molecular structure of the racemic 3mp crystal. The thermal ellipsoids are drawn at the 50% probability level.

Table 3  
Final atomic coordinates and equivalent isotropic thermal parameters for 4mp before irradiation

Atom	x	y	z	$B_{eq}$ or $B$ ( $\text{\AA}^2$ )
Co(1)	0.13161(2)	0.30214(8)	0.59187(9)	3.97(3)
O(1)	0.1614(2)	0.4079(7)	0.3647(7)	7.8(3)
O(2)	0.1521(2)	0.0170(5)	0.7633(6)	7.6(2)
O(3)	0.1054(2)	0.1940(6)	0.8296(7)	7.5(2)
O(4)	0.1135(2)	0.5888(4)	0.4276(6)	7.4(2)
N(1)	0.1611(2)	0.2908(7)	0.4594(7)	5.9(2)
N(2)	0.1567(2)	0.1051(6)	0.6505(7)	5.5(2)
N(3)	0.1044(2)	0.3118(6)	0.7315(6)	5.0(2)
N(4)	0.1087(2)	0.5011(5)	0.5384(6)	4.9(2)
N(5)	0.0620(1)	0.2284(4)	0.3603(5)	3.4(1)
N(6)	0.3021(2)	0.217(1)	0.857(1)	11.9(4)
C(1)	0.1819(2)	0.163(1)	0.467(1)	7.3(4)
C(2)	0.1789(2)	0.0529(8)	0.580(1)	7.0(3)
C(3)	0.0853(2)	0.4381(8)	0.7303(8)	5.8(3)
C(4)	0.0873(2)	0.5506(6)	0.6154(9)	5.5(2)
C(5)	0.2055(3)	0.142(1)	0.362(1)	11.7(5)
C(6)	0.2019(3)	-0.100(1)	0.615(1)	11.5(4)
C(7)	0.0653(3)	0.466(1)	0.843(1)	9.7(4)
C(8)	0.0678(3)	0.7090(8)	0.589(1)	9.6(4)
C(9)	0.0388(2)	0.2928(6)	0.1916(7)	4.2(2)
C(10)	-0.0084(2)	0.2478(7)	0.0373(8)	4.8(2)
C(11)	-0.0345(2)	0.1317(6)	0.0484(7)	4.6(2)
C(12)	-0.0105(2)	0.0625(6)	0.2189(8)	4.9(2)
C(13)	0.0367(2)	0.1119(6)	0.3690(7)	4.4(2)
C(14)	-0.0873(2)	0.0839(8)	-0.1183(8)	7.2(3)
C(15)	0.1973(2)	9.3740(8)	0.8285(8)	7.1(3)
C(16)	0.2403(3)	0.413(1)	0.837(1)	11.1(5)
C(17)	0.2752(3)	0.291(1)	0.853(1)	8.4(4)

$$B_{eq} = \frac{8}{3} \pi^2 \sum_i \sum_j U_{ij} a_i^* a_j^* \mathbf{a}_i \cdot \mathbf{a}_j.$$

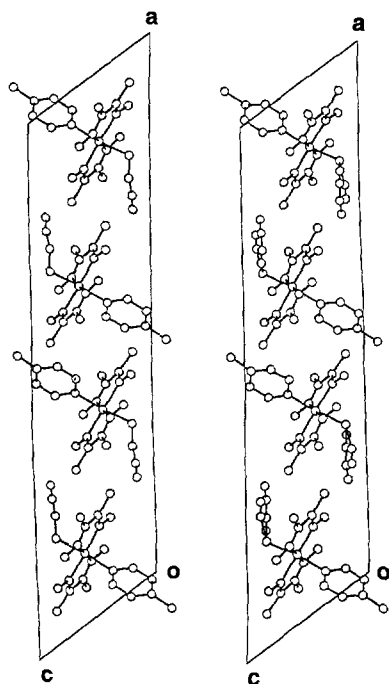


Fig. 7. Crystal structures of 4mp viewed along the  $b$  axis (a) before and (b) after irradiation at 346 K.

Table 4  
Final atomic coordinates and equivalent isotropic thermal parameters for 4mp after irradiation

Atom	x	y	z	$B$ or $B_{eq}$ ( $\text{\AA}^2$ )
Co(1)	0.13196(5)	0.8022(2)	0.5885(2)	4.22(6)
O(1)	0.1622(3)	0.902(1)	0.359(1)	8.2(5)
O(2)	0.1521(3)	0.518(1)	0.760(1)	7.6(4)
O(3)	0.1055(3)	0.701(1)	0.829(1)	7.6(5)
O(4)	0.1137(3)	1.0843(9)	0.420(1)	7.1(4)
N(1)	0.1611(3)	0.787(1)	0.456(1)	5.3(5)
N(2)	0.1570(4)	0.602(1)	0.649(2)	5.5(5)
N(3)	0.1040(3)	0.814(1)	0.726(1)	4.9(4)
N(4)	0.1090(4)	1.000(1)	0.536(1)	4.9(5)
N(5)	0.0620(3)	0.7272(9)	0.358(1)	3.6(4)
N(6A)	0.3011	0.7137	0.8436	11
N(6B)	0.2784	0.7387	0.8814	6
C(1)	0.1821(5)	0.661(2)	0.460(2)	7.5(9)
C(2)	0.1787(5)	0.557(2)	0.571(2)	6.7(8)
C(3)	0.0859(5)	0.939(2)	0.728(2)	5.9(7)
C(4)	0.0865(5)	1.049(1)	0.609(2)	5.5(6)
C(5)	0.2057(5)	0.638(2)	0.358(2)	11(1)
C(6)	0.2012(5)	0.399(2)	0.608(2)	11.4(9)
C(7)	0.056(6)	0.970(2)	0.841(2)	10(1)
C(8)	0.0679(6)	1.206(2)	0.585(2)	9.6(8)
C(9)	0.0374(4)	0.611(1)	0.374(1)	4.2(5)
C(10)	-0.0097(4)	0.561(1)	0.221(2)	4.9(5)
C(11)	-0.0343(4)	0.632(1)	0.055(2)	4.8(5)
C(12)	-0.0084(4)	0.747(1)	0.039(1)	5.1(6)
C(13)	0.0391(4)	0.791(1)	0.194(1)	4.1(4)
C(14)	0.0875(4)	0.580(2)	-0.113(2)	7.6(6)
C(15A)	0.1982	0.8690	0.8364	8.2
C(15B)	0.2508	0.7891	0.8783	12
C(16A)	0.2409	0.9159	0.8337	11
C(17A)	0.2739	0.8082	0.8346	8
C(17B)	0.2181	1.0164	0.8402	9

$$B_{eq} = \frac{8}{3} \pi^2 \sum_i \sum_j U_{ij} a_i^* a_j^* \mathbf{a}_i \cdot \mathbf{a}_j.$$

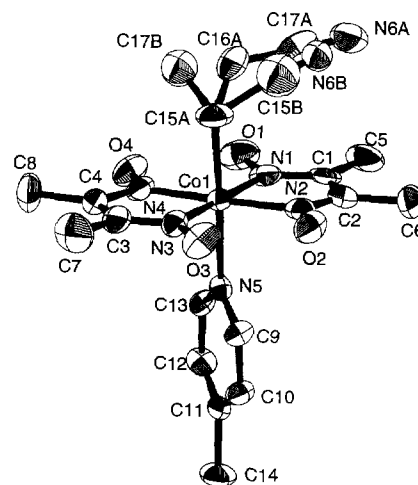


Fig. 8. Molecular structure of 4mp with numbering of atoms after irradiation at 346 K. The thermal ellipsoids are drawn at the 30% probability level. The H atoms are omitted for clarity. The structure before irradiation [14] is approximately the same as that after irradiation, except the produced  $\alpha$ -ce group.

with their estimated standard deviations are given in Tables 3 and 4 respectively. The coordinates before the irradiation are essentially the same as those reported previously at 363 K [14]. The crystal structures before and after the irradiation are compared in Fig. 7. The  $\alpha$ -ce group appeared around the  $\beta$ -ce group. The molecular structure with the numbering atoms after the irradiation is shown in Fig. 8. The produced  $\alpha$ -ce group has an ordered structure and its configuration is *R*. No peaks assigned to the  $\alpha$ -ce group with *S* configuration were observed. The molecular structures before and after the irradiation are not significantly different to each other except the produced  $\alpha$ -ce group. The population of the produced  $\alpha$ -ce and the original  $\beta$ -ce complexes are 0.30 and 0.70 respectively. The bond distances and angles after the irradiation are not significantly different from the corresponding ones determined so far.

#### 4. Discussion

##### 4.1. Generation of asymmetry in the photoisomerization

Fig. 9 shows the molecular structures viewed along the normal to the cobaloxime plane after the irradiation for 3mp and 4mp crystals. Although the conformations of the initial  $\beta$ -ce groups of both crystals are similar to each other, the configuration of the produced  $\alpha$ -ce groups are different; *S* configuration is dominant for 3mp whereas only *R* is produced for 4mp.

In the process of the isomerization, the  $\beta$ -ce radical formed by the homolytic cleavage of the Co–C bond may be transformed to the  $\beta$ -ce radical and then the recombination of the cobalt and the  $\alpha$ -ce radical would produce the  $\alpha$ -ce group. If the produced  $\alpha$ -ce group does not match the surrounding atoms, it would be easily restored to the  $\alpha$ -ce radical. Finally, the ratio of

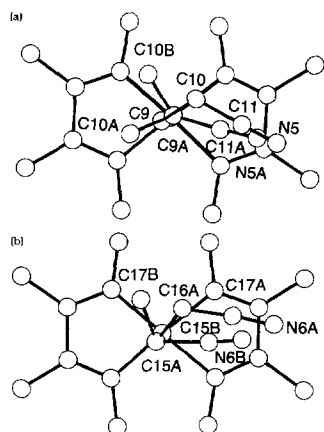


Fig. 9. Conformations of the  $\beta$ - and  $\alpha$ -ce groups viewed along the normal to the cobaloxime plane after the irradiation for (a) 3mp and (b) 4mp molecules. The axial amines are omitted for clarity.

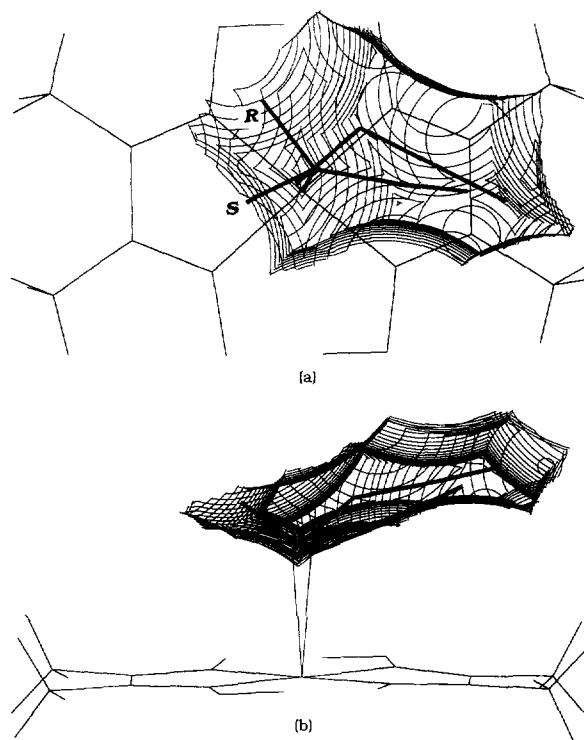


Fig. 10. Reaction cavities for the  $\beta$ -ce group in the 3mp crystal before irradiation: (a) viewed along the normal to the cobaloxime plane; (b) its side view. The initial  $\beta$ -ce and the produced  $\alpha$ -ce groups are indicated in solid lines.

the *R* and *S* configurations should depend on the repulsion with the surrounding atoms in the crystal structure.

We defined the reaction cavity for the reactive group in the crystalline-state racemization [2], in order to estimate the repulsion with surrounding atoms. The reaction cavity for the  $\beta$ -ce group in the 3mp before the irradiation is shown in Fig. 10, in which the produced  $\alpha$ -ce groups as well as the initial  $\beta$ -ce group are also shown. Fig. 11 shows the stereoscopic drawing of the cavity. The space in the cavity at the position of the *R* methyl group is very thin and the methyl group protrudes from the cavity. On the other hand, a large part

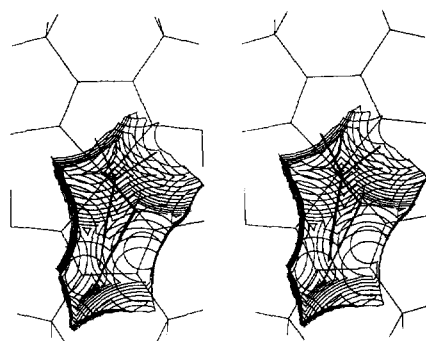


Fig. 11. Stereoscopic drawing of the reaction cavity for the  $\beta$ -ce group in the 3mp crystal.



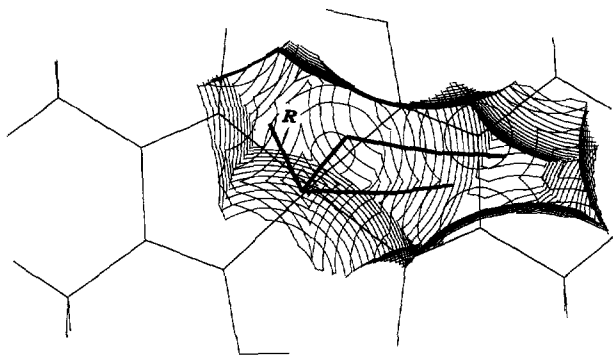


Fig. 12. Reaction cavities for the  $\beta$ -ce group in the 4mp crystal before irradiation viewed along the normal to the cobaloxime plane. The initial  $\beta$ -ce and the produced  $\alpha$ -ce groups are indicated in solid lines.

of the *S* methyl group is included in the cavity, since the cavity around the *S*-methyl group is thicker than that around the *R*-methyl group. The *R*- $\alpha$ -ce group should have higher repulsion with the neighboring atoms than the *S*- $\alpha$ -ce group. This may cause the unequal ratio of the *R* and *S* configurations of the produced  $\alpha$ -ce groups in the 3mp crystal.

Fig. 12 shows the reaction cavity for the  $\beta$ -ce group of 4mp before the irradiation viewed along the normal to the cobaloxime plane. The methyl group of the *R*- $\alpha$ -ce group occupies the very wide space in the cavity whereas the *S*-methyl group has no space. This well explains the reason why only the *R*- $\alpha$ -ce group is produced in the 4mp crystal.

These facts clearly indicate that the asymmetry can be generated from the achiral molecule in a chiral crystal environment. Unfortunately both of the crystals have a centrosymmetric space group. The  $\alpha$ -ce groups with the opposite ratio of *R* and *S* configurations are produced at the inverted site. The optical rotation cannot be observed for these crystals.

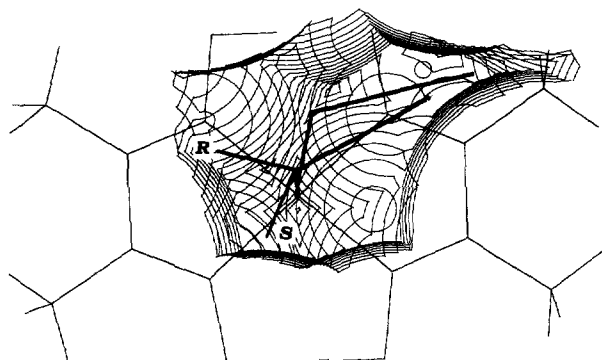


Fig. 13. The reaction cavity for the  $\beta$ -ce group in (*R*)-phenylglycinol crystal viewed along the normal to the cobaloxime plane. The initial  $\beta$ -ce and the produced  $\alpha$ -ce groups are indicated in solid lines.

#### 4.2. Possibility of asymmetric synthesis

The above results suggest that the asymmetric synthesis may be possible if the crystal has a chiral space group. Many attempts to obtain a chiral crystal containing an achiral molecule changing the axial base ligand, however, were unsuccessful. Recently, several  $\beta$ -ce complexes with chiral amines as axial base ligands were prepared. Among the complexes, the powdered sample of the complex with (*R*)-phenylglycinol as an axial base ligand was found to give a very high optical yield (ca. 80%), when it was irradiated with visible light [26]. Fig. 13 shows the cavity for the  $\beta$ -ce group of the complex. It seems clear that the *R*-methyl group has much wider space than the *S*-methyl group, as indicated by dotted lines. This figure suggests that the *R*- $\alpha$ -ce complex should be made predominantly. This is inconsistent with the result obtained in the above powder experiment [26]. Such a high optical yield may indicate that the crystal lattice would be locally retained in the process of the isomerization, although the crystal was gradually decomposed on exposure to an Xe lamp.

These results suggest that although the reaction cavity is very effective in analyzing the reaction mechanism in the solid state reaction, it is necessary to define the asymmetry of the cavity to discuss the asymmetric reaction more quantitatively. Further study is now in progress.

#### Acknowledgements

This work was supported by a Grant-in-Aid for Scientific Research on Priority Area No. 06227225 from the Ministry of Education, Science and Culture, Japan.

#### References

- [1] Y. Ohashi, Y. Sasada, *Nature* 267 (1977) 142.
- [2] Y. Ohashi, K. Yanagi, T. Kurihara, Y. Sasada, Y. Ohgo, *J. Am. Chem. Soc.* 103 (1981) 5805.
- [3] Y. Ohashi, *Acc. Chem. Res.* 21 (1988) 268.
- [4] Y.T. Osano, A. Uchida, Y. Ohashi, *Nature* 352 (1991) 510.
- [5] Y. Ohashi, T. Nemoto, Y. Takenaka, *Mol. Cryst. Liq. Cryst.* 242 (1994) 103.
- [6] Y. Ohgo, S. Takeuchi, *J. Chem. Soc. Chem. Commun.* (1985) 21.
- [7] A. Uchida, M. Danno, Y. Sasada, Y. Ohashi, *Acta Crystallogr. Sect. B*: 43 (1987) 528.
- [8] A. Uchida, Y. Ohashi, *Acta Crystallogr. Sect. C*: 47 (1991) 1177.
- [9] A. Sekine, Y. Ohashi, E. Shimizu, K. Hori, *Acta Crystallogr. Sect. C*: 47 (1991) 53.
- [10] A. Sekine, Y. Ohashi, K. Hori, *Acta Crystallogr. Sect. C*: 47 (1991) 525.

- [11] Y. Ohashi, A. Sekine, E. Shimizu, K. Hori, A. Uchida, *Mol. Cryst. Liq. Cryst.* 186 (1990) 37.
- [12] A. Sekine, Y. Ohashi, *Bull. Chem. Soc. Jpn.* 64 (1991) 2183.
- [13] A. Uchida, Y. Ohashi, Y. Sasada, *Nature* 320 (1986) 51.
- [14] A. Uchida, Y. Sasada, Y. Ohashi, *Acta Crystallogr. Sect. B*: 44 (1988) 249.
- [15] L. Addadi, J. van Mill, M. Lahav, *J. Am. Chem. Soc.* 104 (1982) 3422.
- [16] A. Sekine, K. Hori, Y. Ohashi, M. Yagi, F. Toda, *J. Am. Chem. Soc.* 111 (1989) 697.
- [17] C.-M. Chung, M. Hasegawa, *J. Am. Chem. Soc.* 113 (1991) 7311.
- [18] A.D. Gudmundsdottir, J.R. Scheffer, J. Trotter, *Tetrahedron Lett.* 35 (1994) 1397.
- [19] G.N. Schrauzer, R.J. Windgassen, *J. Am. Chem. Soc.* 89 (1967) 1999.
- [20] Y. Ohgo, S. Takeuchi, Y. Natori, J. Yoshimura, Y. Ohashi, Y. Sasada, *Bull. Chem. Soc. Jpn.* 54 (1981) 3095.
- [21] C.J. Gilmore, *J. Appl. Crystallogr.* 17 (1984) 42.
- [22] G. Sheldrick, *SHELXL93*, Program for the Refinement of Crystal Structure, University of Göttingen, Germany.
- [23] *TEXSAN*, Texray Structure Analysis Package, 1985 (Molecular Structure Corporation, 3200 Research Forest Drive, The Woodlands, TX 77381, USA).
- [24] *International Tables for X-ray Crystallography*, Vol. IV, Kynoch Press, Birmingham, UK, 1974 (present distributor Kluwer Academic Publishers, Dordrecht).
- [25] A. Sekine, H. Tatsuki, Y. Ohashi, in preparation.
- [26] Y. Ohgo, Y. Arai, M. Hagiwara, S. Takeuchi, H. Kogo, A. Sekine, Y. Ohashi, *Chem. Lett.* (1994) 715.